Transcriptional activation and phosphorylation of OsCNGC9 confer enhanced chilling tolerance in rice

Jiachang Wang[1,2,5], Yulong Ren[2,5], Xi Liu[1,5], Sheng Luo[2], Xiao Zhang[1], Xin Liu[2], Qibing Lin[2], Shanshan Zhu[2], Hua Wan[1], Yang Yang[3], Yu Zhang[1], Bin Lei[2], Chunlei Zhou[1], Tian Pan[1], Yongfei Wang[1], Mingming Wu[1], Ruonan jing[1], Yang Xu[1], Meng Han[4], Fuqing Wu[2], Cailin Lei[2], Xiuping Guo[2], Zhijun Cheng[2], Xiaoming Zheng[2], Yihua Wang[1], Zhigang Zhao[1], Ling Jiang[1], Xin Zhang[2], Yong-Fei Wang[3], Haiyang Wang[2] and Jianmin Wan[1,2,*]

[1]National Key Laboratory for Crop Genetics and Germplasm Enhancement, Jiangsu Plant Gene Engineering Research Center, Nanjing Agricultural University, Nanjing 210095, China

[2]National Key Facility for Crop Gene Resources and Genetic Improvement, Institute of Crop Sciences, Chinese Academy of Agricultural Sciences, Beijing 100081, China

[3]National Key Laboratory of Plant Molecular Genetics, Institute of Plant Physiology and Ecology, CAS Center for Excellence in Molecular Plant Sciences, Chinese Academy of Sciences, Shanghai 200032, China

[4]MOE Key Laboratory of Bioinformatics, School of Life Sciences, Tsinghua University, Beijing, 100084, China

[5]These authors contributed equally to this article.

*Correspondence: Jianmin Wan (wanjm@njau.edu.cn, wanjianmin@caas.cn)

https://doi.org/10.1016/j.molp.2020.11.022

ABSTRACT

Low temperature is a major environmental factor that limits plant growth and productivity. Although transient elevation of cytoplasmic calcium has long been recognized as a critical signal for plant cold tolerance, the calcium channels responsible for this process have remained largely elusive. Here we report that OsCNGC9, a cyclic nucleotide-gated channel, positively regulates chilling tolerance by mediating cytoplasmic calcium elevation in rice (*Oryza sativa*). We showed that the loss-of-function mutant of *OsCNGC9* is defective in cold-induced calcium influx and more sensitive to prolonged cold treatment, whereas *OsCNGC9* overexpression confers enhanced cold tolerance. Mechanistically, we demonstrated that in response to chilling stress, OsSAPK8, a homolog of *Arabidopsis thaliana* OST1, phosphorylates and activates OsCNGC9 to trigger Ca^{2+} influx. Moreover, we found that the transcription of *OsCNGC9* is activated by a rice dehydration-responsive element-binding transcription factor, OsDREB1A. Taken together, our results suggest that OsCNGC9 enhances chilling tolerance in rice through regulating cold-induced calcium influx and cytoplasmic calcium elevation.

Key words: OsCNGC9, OsSAPK8, OsDREB1A, cold signaling transduction, chilling tolerance

INTRODUCTION

Cold stress is a major environmental stress that limits the growing season and geographical distribution of plants in nature, frequently hampering crop production (Lesk et al., 2016; Zhu, 2016). Rice (*Oryza sativa*), a primary staple crop for more than half of the world's population, was domesticated in temperate areas and is sensitive to chilling stress (Sasaki and Burr, 2000; Zhang et al., 2019). Therefore, improvement of rice chilling

tolerance could reduce cold-induced yield loss and enable the expansion of rice cultivation. Previous studies have shown that cold stress induces the expression of cold-regulated (*COR*) genes by C-repeat (CRT)-binding factors (CBFs)/dehydration-responsive element (DRE)-binding transcription factors (DREBs).

CBFs/DREBs can bind to the CRT/DRE *cis* elements in the promoters of cold-regulated (*COR*) genes and activate a set of *COR* genes, leading to enhanced cold tolerance (Stockinger et al., 1997; Jaglo-Ottosen et al., 1998; Liu et al., 1998; Thomashow, 1999).

It was recently shown that protein kinases play an important role in the regulation of plant cold signaling transduction (Barrero-Gil and Salinas, 2013). For example, OPEN STOMATA 1 (OST1), a member of the SNF1-related protein kinase 2 (SnRK2) family, positively regulates cold tolerance in *Arabidopsis thaliana* (Ding et al., 2015). During cold stress, cold-activated OST1 interacts with and phosphorylates INDUCER OF CBF EXPRESSION 1 (ICE1) to prevent its 26S proteasome-mediated degradation and thus promote its binding activity to CBF proteins (Ding et al., 2015). Moreover, OST1 also phosphorylates basic transcription factor 3s (BTF3s) and promotes CBF protein stability by interacting with CBF proteins (Ding et al., 2018). Consistent with this finding, the *ost1* mutant shows sensitivity to cold stress, whereas *OST1* overexpression transgenic lines show increased cold tolerance (Ding et al., 2015). Although previous studies have shown that OST1 is a key regulator of cold signaling transduction in *Arabidopsis*, little is known about the precise role of SnRK2s in cold signaling transduction in rice.

Ca^{2+}, an important second messenger, has been shown to be involved in plant response to environmental changes, including cold stress (Knight et al., 1996; Yuan et al., 2018). Exposure to cold stress induces a rapid and transient increase in cytoplasmic calcium concentration ($[Ca^{2+}]_{cyt}$), which triggers downstream cold tolerance responses in plants (Sanders et al., 2002; Guo et al., 2018). Furthermore, it has been demonstrated that Ca^{2+} influx from the apoplast is critical for the cold-induced $[Ca^{2+}]_{cyt}$ burst (Carpaneto et al., 2007; Ma et al., 2015); however, the calcium-permeable channels responsible for cold-induced Ca^{2+} influx in plants remain largely unknown (Ding et al., 2019). Recently, CHILLING TOLERANCE DIVERGENCE 1 (COLD1), a plasma membrane and endoplasmic reticulum-localized transmembrane protein, was shown to work together with G-protein α subunit 1 (RGA1) to mediate cold-induced Ca^{2+} influx to promote cold stress tolerance in rice. Although it has been proposed that COLD1 may function as a Ca^{2+}-permeable channel or a subunit of the Ca^{2+} channel (Ma et al., 2015; Manishankar and Kudla, 2015), its exact molecular function still remains to be elucidated.

Cyclic nucleotide-gated channels (CNGCs), a kind of Ca^{2+}-permeable nonspecific cation channel, have been demonstrated to play a crucial role in thermal sensing and thermotolerance in *Arabidopsis* and *Physcomitrella patens* (Finka et al., 2012; Gao et al., 2012; Tunc-Ozdemir et al., 2013). In plants, CNGC-mediated Ca^{2+} signaling has been shown to participate in the regulation of various signaling pathways (DeFalco et al., 2016a). We recently showed that the plasma membrane-localized channel protein OsCNGC9, a Ca^{2+}-permeable nonspecific cation channel, mediates Ca^{2+} influx in rice innate immunity (Wang et al., 2019). In this study, we provide evidence that OsCNGC9 also positively regulates rice chilling tolerance by mediating Ca^{2+} influx in response to chilling stress. We further demonstrate that OsSAPK8, a homolog of *Arabidopsis* OST1, physically interacts with and phosphorylates OsCNGC9 to enhance its channel activity. In addition, a rice DREB transcription factor,

OsDREB1A, can directly bind to the promoter region of *OsCNGC9* to promote its transcription. Here, we reveal that a regulatory pathway composed of OsDREB1A, OsSAPK8, and OsCNGC9 plays a positive role in cold-induced cytoplasmic calcium elevation and chilling tolerance in rice.

RESULTS

OsCNGC9 is a positive regulator of chilling tolerance

A recent study showed that the expression of *OsCNGC9* was significantly induced in response to cold stress (Nawaz et al., 2014). To investigate whether *OsCNGC9* contributes to chilling tolerance in rice, we examined the chilling tolerance of wild type (WT) and *cds1* (*cell death and susceptible to blast 1*), a loss-of-function mutant of *OsCNGC9* (Wang et al., 2019). After a 4-day chilling treatment and a 7-day recovery, only ~10% of the *cds1* seedlings survived, in contrast to ~92% of the WT plants (Figure 1). In addition, two independent *cds1* complementation lines expressing *OsCNGC9::OsCNGC9* (*pGOsCNGC9*; Wang et al., 2019) completely rescued the chilling tolerance defect of the *cds1* mutant (Supplemental Figures 1 and 2A). Furthermore, no significant difference in thermotolerance was detected between WT and *cds1* (Supplemental Figure 3), indicating that heat-shock signaling may be independent of OsCNGC9. Together, these results suggest that *OsCNGC9* is involved in rice chilling tolerance.

We next investigated whether *OsCNGC9* could mediate Ca^{2+} influx in response to chilling shock *in vivo* using Non-invasive Micro-test Technology (NMT) in rice roots (Ma et al., 2015). Upon chilling stimulation, there was a rapid and robust extracellular Ca^{2+} influx in the roots of WT and the complementation lines of *cds1*. By contrast, *cds1* showed no significant extracellular Ca^{2+} influx under the same conditions (Figure 2A). We also observed that the maximum Ca^{2+} influx under cold stress differed significantly between *cds1* and WT or *pGOsCNGC9* (Figure 2B). In addition, we used Yellow Cameleon 3.6 (YC3.6) as a ratiometric fluorescent calcium indicator to further monitor $[Ca^{2+}]_{cyt}$ elevation during cold stress (Behera et al., 2015). The root cells of WT and *pGOsCNGC9* showed very significant cytoplasmic Ca^{2+} elevation after cold treatment, whereas those of *cds1* showed relatively weaker cytoplasmic Ca^{2+} elevation in response to cold shock (Figure 2C and 2D). Moreover, similar results were observed when Fluo-4 acetoxymethyl (AM) ester was used as a fluorescent $[Ca^{2+}]_{cyt}$ indicator (Supplemental Figure 4). Furthermore, qRT–PCR analysis showed that in response to chilling stimulation, the induction levels of cold stress-related calcium-dependent protein kinase genes (*CPKs*) and *OsDREB1A* were significantly lower in *cds1* than in WT and the *cds1* complementation lines (Figure 2E–2G). On the other hand, the expression of *OsTT1* (a heat stress-related gene) was not obviously induced by cold stress (Figure 2H), and heat stress-induced Ca^{2+} influx was not affected in *cds1* compared with WT plants (Supplemental Figure 5). These results suggest that *OsCNGC9* participates in the regulation of chilling tolerance by mediating chilling-induced Ca^{2+} influx in rice.

To further assess the role of *OsCNGC9* in rice chilling tolerance, we examined the chilling tolerance of *OsCNGC9*-overexpression (*OsCNGC9-OE*) transgenic lines in the *japonica* rice Kitaake
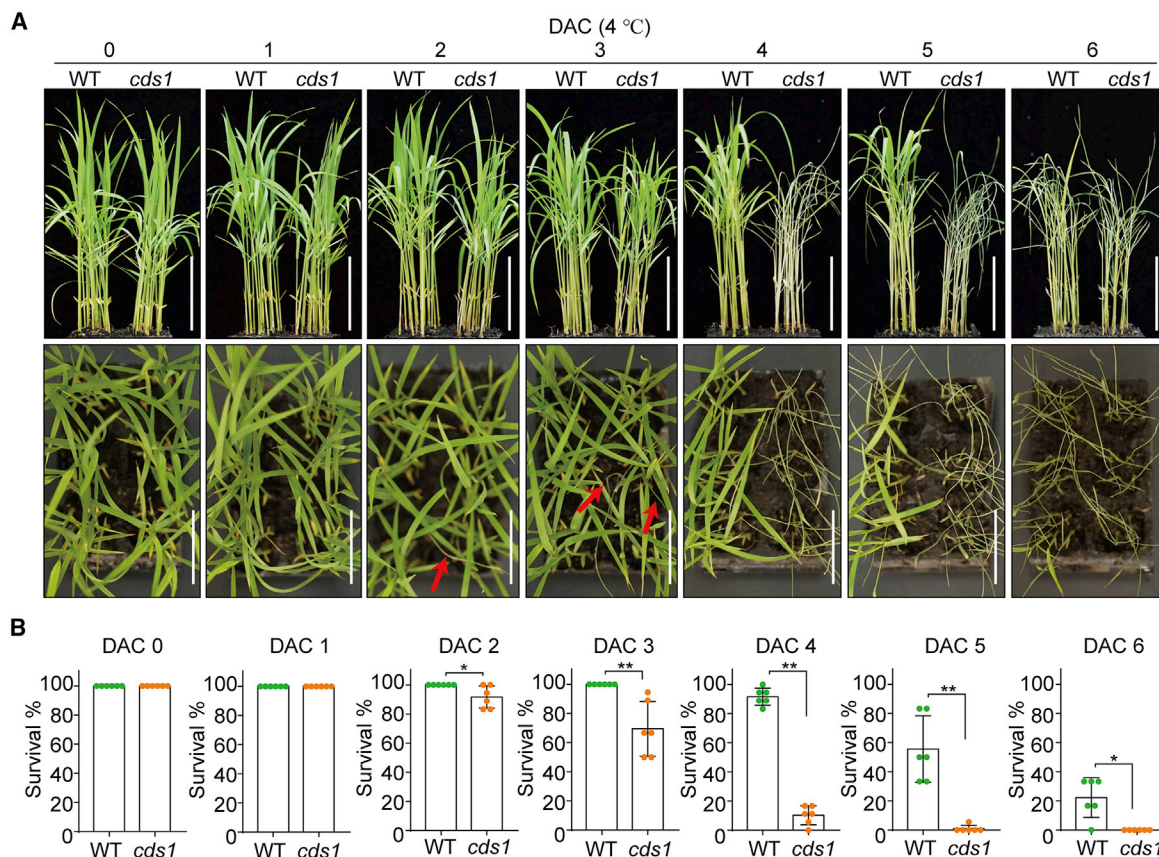
Figure 1. OsCNGC9 positively regulates chilling tolerance in rice seedlings.

(A) Chilling tolerance phenotype of wild-type **(**WT) and *cds1* plants. Seedlings were incubated at 4°C for the indicated days and then transferred back to the normal temperature for 7 days of recovery. Shown are the front view (upper panel) and the vertical view (lower panel) of WT and *cds1* plants before and after chilling treatment. Red arrows indicate dead plants. Scale bars, 5 cm.

(B) The survival rate was measured after chilling treatment for the indicated number of days and recovery for 7 days. Values are means ± SD, $n = 6$ (six technical replicates per biological repeat, with at least 18 seedlings per technical replicate). *$P < 0.05$, **$P < 0.01$ (compared with WT; Student's *t-test*). DAC, days after chilling treatment.

The experiments were repeated three times with similar results.

background (Wang et al., 2019). *OsCNGC9-OE* transgenic seedlings showed significantly higher survival rates than Kitaake after chilling treatment (Supplemental Figures 2B and 6). Moreover, Ca^{2+} flux and cytoplasm Ca^{2+} assays showed that the *OsCNGC9-OE* lines exhibited stronger extracellular Ca^{2+} influx and greater $[Ca^{2+}]_{cyt}$ elevation than Kitaake in response to chilling shock (Supplemental Figure 7A–7C). In addition, a qRT–PCR assay showed that the *OsCNGC9-OE* lines exhibited higher cold stress-related gene expression than Kitaake after cold treatment (Supplemental Figure 7D and 7E). Taken together, these results suggest that *OsCNGC9* positively regulates chilling tolerance by mediating Ca^{2+} influx in rice.

OsCNGC9 physically interacts with OsSAPK8

To elucidate the regulatory mechanism of *OsCNGC9* in chilling tolerance, we sought to identify OsCNGC9-interacting proteins. The OsCNGC9-GFP fusion protein or free GFP protein was transiently expressed in rice protoplasts, followed by immunoprecipitation using anti-GFP beads and liquid chromatography–tandem mass spectrometry (LC–MS/MS). Interestingly, one candidate protein identified in protoplasts expressing OsCNGC9-GFP, but not in control protoplasts expressing free GFP, was OsSAPK8, a SnRK2

protein kinase (Kobayashi et al., 2004; Sun et al., 2016) (Supplemental Table 1). A very recent study has revealed that OsSAPK8 functions as a positive regulator in response to abiotic stresses, including cold stress (Zhong et al., 2020). In addition, OST1, the homolog of rice OsSAPK8, plays a crucial role in the cold tolerance of *Arabidopsis* (Ding et al., 2015, 2018). We therefore verified the interaction between OsSAPK8 and OsCNGC9 using multiple assays. A yeast two-hybrid (Y2H) assay showed that OsSAPK8 could directly interact with OsCNGC9 (Figure 3A). A split-luciferase complementation assay in *Nicotiana benthamiana* showed that the co-expression of cLUC-OsCNGC9 and nLUC-OsSAPK8 produced an obvious luciferase (LUC) signal (Figure 3B). Furthermore, a co-immunoprecipitation (CoIP) assay in rice protoplasts confirmed that OsSAPK8 could be co-immunoprecipitated with OsCNGC9-GFP using anti-GFP beads (Figure 3C). Together, these results suggest that OsSAPK8 physically interacts with OsCNGC9 *in vivo*.

OsSAPK8 phosphorylates OsCNGC9 to enhance its Ca^{2+} channel activity

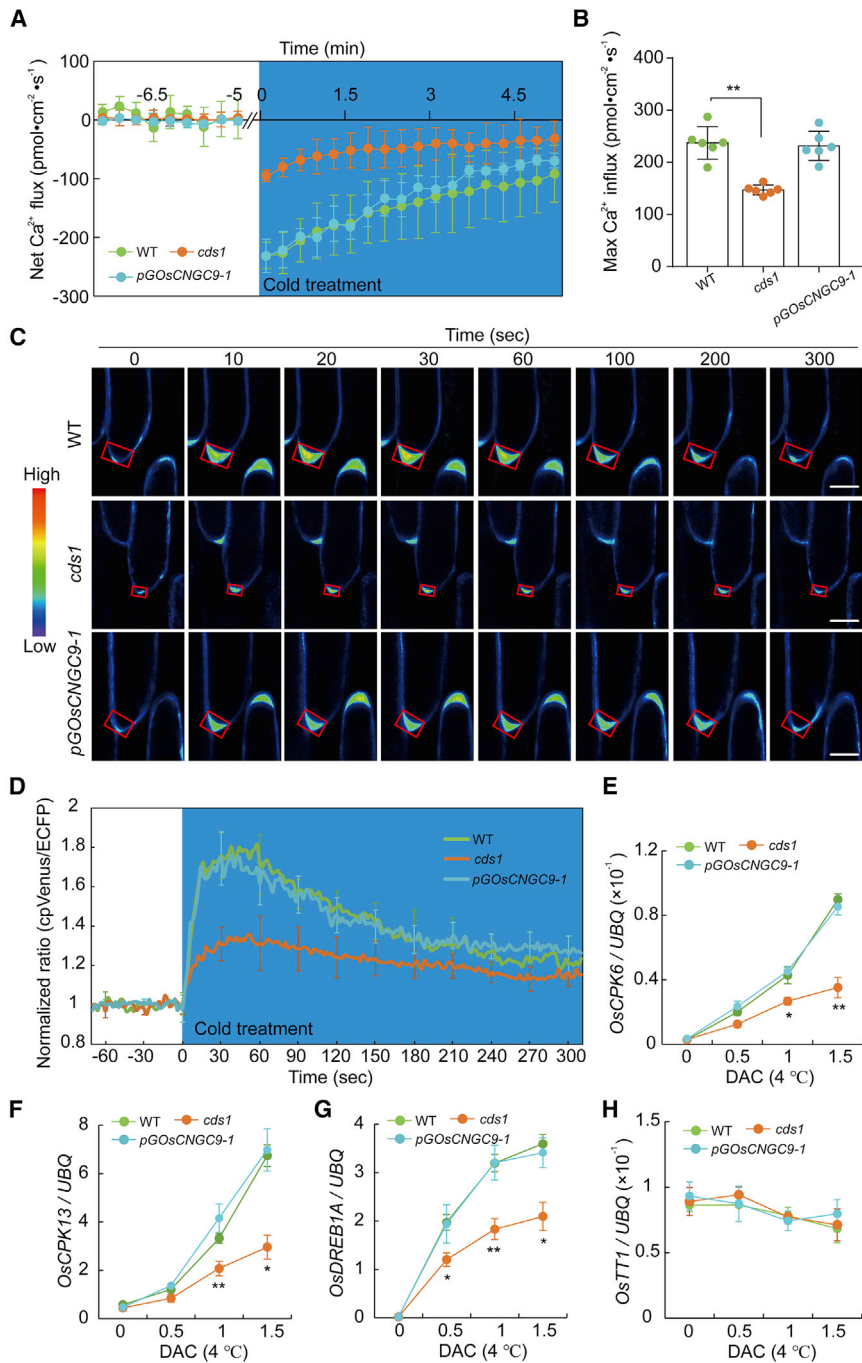The observed physical interaction between OsSAPK8 and OsCNGC9 prompted us to further investigate whether OsCNGC9

Figure 2. OsCNGC9 is required for cold-induced Ca²⁺ influx and cold stress-related gene expression.

(A) Comparison of extracellular calcium influx in living roots of wild type (WT), *cds1*, and *pGOsCNGC9* transgenic plants upon cold shock. The blue background indicates the duration of cold treatment.

(B) Calculated maximum Ca²⁺ influxes from **(A)**. Values are means ± SD ($n = 6$, compared with WT; **$P < 0.01$, Student's *t-test*).

(C) Cold-induced $[Ca^{2+}]_{cyt}$ accumulation in live root cells using Yellow Cameleon (NES-YC3.6). The red rectangles represent regions of interest (ROIs) used for ratiometric measurements. Ratio images were acquired at the indicated times. The $[Ca^{2+}]_{cyt}$ responses were visualized using a color gradient from low (blue) to high (red). Scale bars, 10 μm.

(D) Normalized ratio (cpVenus/ECFP) values showing $[Ca^{2+}]_{cyt}$ changes upon cold treatment in the live root cells of WT, *cds1*, and *pGOsCNGC9* transgenic plants. The blue background indicates the duration of cold treatment. Scale bars, 10 μm. Values are means ± SD ($n = 6$). Error bars are indicated every 30 s for clarity. The experiments were replicated at least three times.

(E–H) Dynamic change in the expression levels of cold stress-related genes (*OsCPK6*, *OsCPK13*, and *OsDREB1A*) and the heat stress-related gene *OsTT1* in WT, *cds1*, and *pGOsCNGC9* transgenic plants in response to cold stress. Values are means ± SD ($n = 3$, compared with WT; *$P < 0.05$, **$P < 0.01$, Student's *t-test*).

All experiments were repeated three times with similar results.

is a substrate of OsSAPK8. Previous studies have revealed that phosphorylation of the C terminus of plant CNGCs is involved in their regulation (He et al., 2019; Tian et al., 2019; Wang et al., 2019; Yu et al., 2019). Consistent with this finding, our Y2H assay showed that OsCNGC9 interacts with OsSAPK8 via its C terminus (Supplemental Figure 8). Therefore, we next examined whether OsSAPK8 could phosphorylate the C terminus of OsCNGC9 (OsCNGC9-C) using an *in vitro* phosphorylation assay. A Phos-tag SDS–PAGE assay showed that OsCNGC9-C was clearly phosphorylated by OsSAPK8 (Figure 3D). To examine whether OsCNGC9 is phosphorylated during cold stress *in planta*, we performed an *in vivo* phosphorylation

assay. Indeed, the phosphorylation level of OsCNGC9-C was markedly increased within minutes after cold treatment (Figure 3E). Next, we examined whether OsCNGC9 is phosphorylated in an OsSAPK8-dependent manner during cold stress *in planta* by comparing the phosphorylation level of OsCNGC9-C in the *OsSAPK8* knockout line (*OsSAPK8-KO*; Supplemental Figure 9) with that in the corresponding WT, Nipponbare. The relative phosphorylation intensity of OsCNGC9-C was induced to a lesser extent in protoplasts from the *OsSAPK8-KO* knockout plants than in those from Nipponbare after cold shock (Figure 3F). Together, these results suggest that OsCNGC9 is an authentic substrate of OsSAPK8.

To elucidate the role of phosphorylation by OsSAPK8 on the Ca²⁺ channel activity of OsCNGC9, we performed a calcium imaging assay in HEK293T cells. After treatment with 10 mM external CaCl₂, HEK293T cells co-expressing *OsSAPK8* and *OsCNGC9* showed a stronger increase in cytosolic Ca²⁺ than HEK293T cells expressing *OsCNGC9* alone (Figure 3G–3I). In addition, no significant cytosolic Ca²⁺ increase was observed in intact HEK293T cells expressing *OsSAPK8* alone
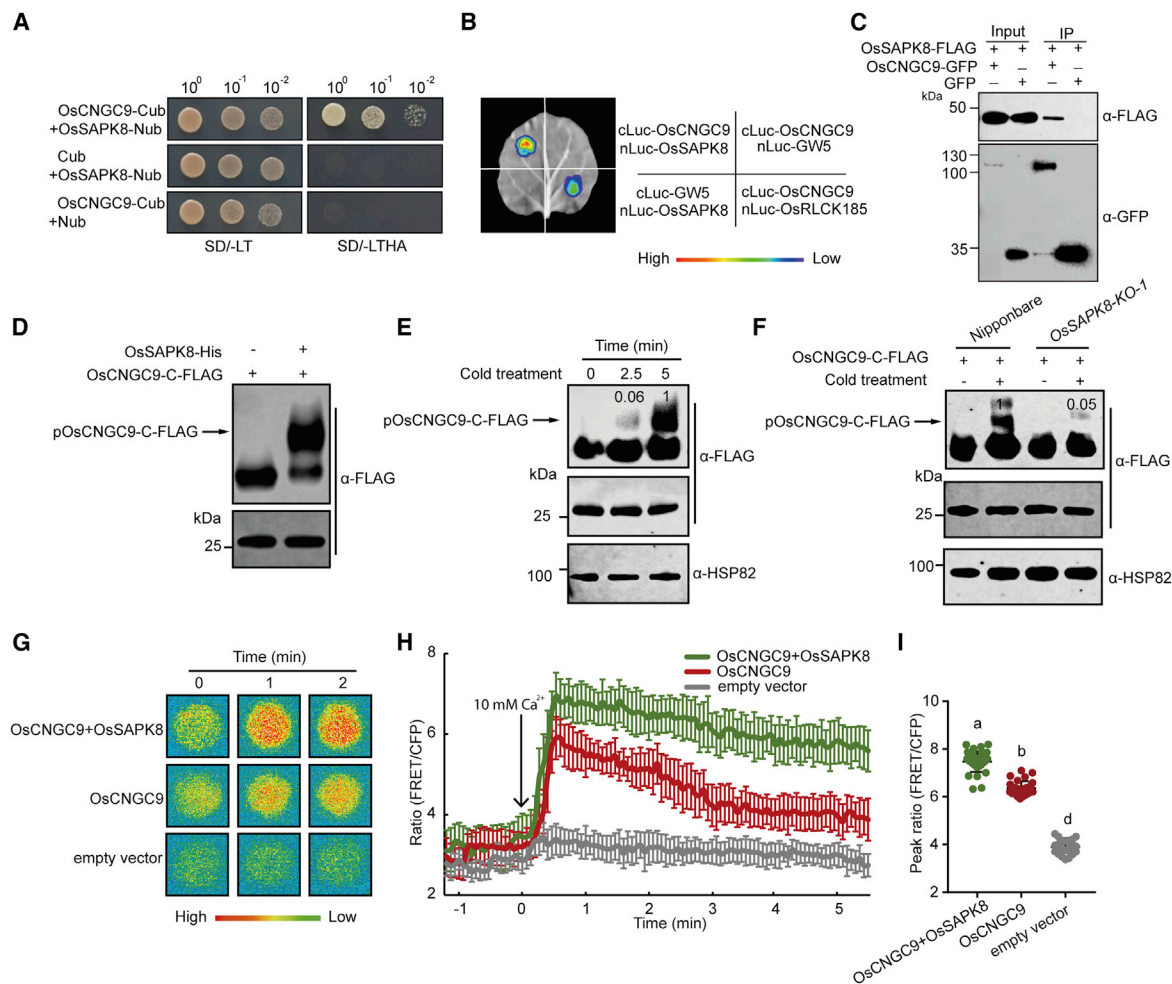
Figure 3. OsSAPK8 physically interacts with and phosphorylates OsCNGC9 to enhance its channel activity.

(A) Yeast two-hybrid assay showing the interaction between OsCNGC9 and OsSAPK8. SD/-LT, Synthetic Dropout/-Leu-Trp; SD/-LTHA, Synthetic Dropout/-Leu-Trp-His-Ade.

(B) Split-luciferase complementation assay showing the interaction between OsCNGC9 and OsSAPK8 in *N. benthamiana* leaves. GW5 was used as a negative control, and OsRLCK185 was used as a positive control in the LUC assay. cLUC, C terminus of LUC; nLUC, N terminus of LUC.

(C) Co-immunoprecipitation (Co-IP) of OsCNGC9 and OsSAPK8 in rice protoplasts. The plus (+) and minus (−) signs denote the presence and absence of the protein in each sample.

(D) *In vitro* phosphorylation assay showing that the C terminus of OsCNGC9 (OsCNGC9-C) is phosphorylated by OsSAPK8. The phosphorylation of OsCNGC9-C was examined using a Phos-tag SDS–PAGE assay (upper panel) and SDS–PAGE (lower panel).

(E) Cold stress induces OsCNGC9-C phosphorylation *in vivo*. Protein extracts from rice protoplasts expressing *OsCNGC9-C-FLAG* were separated in a Phos-tag gel (upper panel) and SDS–PAGE (lower panel), and then detected with the indicated antibodies. The relative intensity of each shifted phosphorylated band is indicated.

(F) *In vivo* phosphorylation assay of OsCNGC9-C under cold stress in Nipponbare and the *OsSAPK8-KO* plants. Protein extracts from Nipponbare and *OsSAPK8-KO* protoplasts expressing *OsCNGC9-C-FLAG* were treated with or without cold stress for 5 min before protein extraction. The relative intensity of shifted phosphorylated bands is indicated. The plus (+) and minus (−) signs denote the presence or absence of the protein in each sample. The relative intensity of each shifted phosphorylated band is indicated.

(G–I) Ca^{2+} imaging in HEK293T cells showing the activation of OsCNGC9 by OsSAPK8 and the consequent increase in [Ca^{2+}]$_{cyt}$. Typical fluorescent images **(G)**, average fluorescence intensity changes **(H)**, and peak fluorescence intensity **(I)** in HEK293T cells transiently expressing various tested proteins are indicated. The [Ca^{2+}]$_{cyt}$ responses were visualized using a color gradient from low (blue) to high (red). Values are means ± SD ($n \geq 30$; $P \leq 0.05$, Student's *t*-test). Significant differences are indicated by different lowercase letters.

All experiments were repeated three times with similar results.

(Supplemental Figure 10). These results suggest that OsSAPK8 was able to activate OsCNGC9 channel activity. The above data collectively suggest that the phosphorylation of OsCNGC9 by OsSAPK8 enhances OsCNGC9 channel activity in response to cold stress.

Phosphorylation of OsCNGC9-Ser645 enhances chilling tolerance in rice

To identify phospho-sites in OsCNGC9-C before and after cold shock, we expressed an OsCNGC9-C-FLAG fusion protein in rice protoplasts and then treated them with or without cold stress.
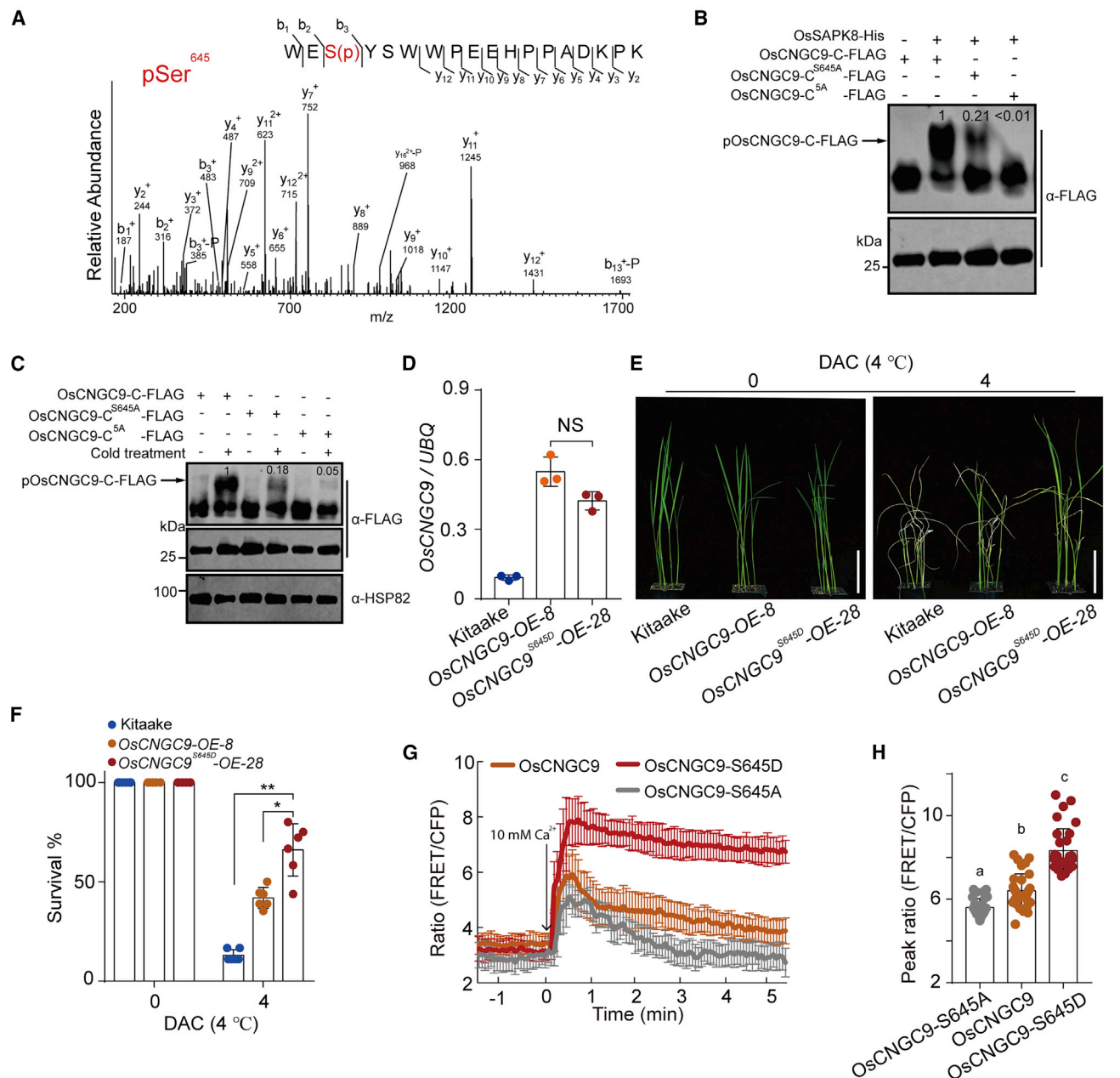
Figure 4. The Ser645 phosphorylation of OsCNGC9 plays a positive role in rice chilling tolerance.

(A) LC–MS/MS analysis revealed that OsCNGC9 Ser645 is phosphorylated by OsSAPK8.

(B) *In vitro* phosphorylation assay showed that the Ser645A mutant of OsCNGC9-C (OsCNGC9-C^{S645A}) and the Ser^{541A}/Ser^{576A}/Ser^{639A}/Ser^{645A}/Ser^{674A} quintuple mutant of OsCNGC9-C (OsCNGC9-C^{5A}) exhibit compromised phosphorylation by OsSAPK8. Proteins were fractionated by SDS–PAGE containing Phos-tag acrylamide (upper panel) and normal SDS–PAGE (lower panel). The relative intensity of shifted phosphorylated bands is indicated. The plus (+) and minus (−) signs denote the presence and absence of the protein in each sample. The relative intensity of each shifted phosphorylated band is indicated.

(C) *In vivo* phosphorylation assay of OsCNGC9-C, OsCNGC9-C^{S645A}, and OsCNGC9-C^{5A} under cold stress in Nipponbare protoplasts. Protein extracts from Nipponbare protoplasts expressing *OsCNGC9-C-FLAG*, *OsCNGC9-C^{S645A}-FLAG*, and *OsCNGC9-C^{5A}-FLAG* were treated with or without cold stress for 5 min before protein extraction. The relative intensity of shifted phosphorylated bands is indicated. The plus (+) and minus (−) signs denote the presence and absence of the protein in each sample. The relative intensity of each shifted phosphorylated band is indicated.

(D) Expression level of *OsCNGC9* in the leaves of Kitaake, *OsCNGC9-OE* transgenic plants, and the phosphomimetic *OsCNGC9* transgenic plants (*OsCNGC9^{S645D}-OE*). WT *OsCNGC9* or *OsCNGC9^{S645D}* was overexpressed in Kitaake, and T2 transgenic lines were used to examine the expression level of *OsCNGC9*. Values are means ± SD ($n = 3$; NS, not significant, Student's *t*-test).

(E) The chilling tolerance of phosphomimetic *OsCNGC9* mutants is significantly enhanced. Seedlings were incubated at 4°C for the indicated days and then transferred back to the normal temperature for 7 days of recovery. DAC, days after cold treatment. Scale bars, 5 cm.

The OsCNGC9-C-FLAG protein was enriched by affinity purification and then subjected to LC–MS/MS analysis. Five specific phospho-sites were identified in OsCNGC9-C purified from the protoplasts treated with chilling shock (Supplemental Figure 11). Strikingly, Ser645 of OsCNGC9 showed the highest phosphorylation intensity after the chilling treatment among all identified phospho-sites (Figure 4A and Supplemental Table 2), indicating that Ser645 is likely a major phosphorylation site under chilling conditions *in vivo*. Amino acid sequence analysis showed that Ser645 is located in the RXXS/T domain that is specifically recognized by SnRK2 kinases (Supplemental Figure 11; Kobayashi et al., 2005). To determine whether OsSAPK8 phosphorylates OsCNGC9 at Ser645, we conducted an *in vitro* phosphorylation assay. OsSAPK8-phosphorylated OsCNGC9-C-FLAG protein was subjected to LC–MS/MS assay. We also identified multiple confident OsSAPK8 phosphorylation sites on OsCNGC9-C (Supplemental Figure 11). Consistently, the phosphorylation intensity of Ser645 was the highest among all identified OsSAPK8 phosphorylation sites on OsCNGC9 (Supplemental Table 3). Site-directed mutagenesis showed that the substitution of Ser645 with Ala (OsCNGC9-C^{S645A}) significantly reduced OsCNGC9-C phosphorylation by OsSAPK8, and the Ser^{541A}Ser^{576A}Ser^{639A}Ser^{645A}Ser^{674A} quintuple mutant (OsCNGC9-C^{5A}) almost completely lacked OsSAPK8-dependent phosphorylation *in vitro* (Figure 4B). Similarly, we found that cold stress-induced phosphorylation of OsCNGC9 was weakened in protoplasts expressing *OsCNGC9-C^{S645A}* and was almost completely lost in protoplasts expressing the Ser^{541A}Ser^{576A}Ser^{639A}Ser^{645A}Ser^{674A} quintuple mutant (Figure 4C). Together, these results suggest that Ser645 of OsCNGC9 is a major site of phosphorylation by OsSAPK8 in response to chilling stress in rice.

To elucidate the role of OsCNGC9 Ser645 in rice chilling tolerance, we generated phosphomimetic *OsCNGC9-S645D* overexpression (*OsCNGC9^{S645D}-OE*) transgenic lines. We selected *OsCNGC9-OE* and *OsCNGC9^{S645D}-OE* transgenic lines with similar *OsCNGC9* expression levels and compared their chilling tolerance (Figure 4D). After chilling treatment and recovery, the survival rate of *OsCNGC9^{S645D}-OE* plants was greater than 65%, whereas that of *OsCNGC9-OE* plants was only about 40% under the same conditions (Figure 4E and 4F; Supplemental Figure 2C). Together, these results suggest that the phosphorylation of OsCNGC9 Ser645 by OsSAPK8 enhances chilling tolerance in rice.

To further verify whether the phosphorylation status of OsCNGC9 Ser645 affects the channel activity of OsCNGC9, we performed a calcium imaging assay using OsCNGC9, OsCNGC9^{S645D}, and OsCNGC9^{S645A}. As shown in Figure 4G and 4H, cytosolic Ca^{2+} elevation was significantly enhanced in intact HEK293T cells expressing *OsCNGC9^{S645D}* compared with those expressing *OsCNGC9* upon the application of 10 mM external CaCl$_2$. By contrast, HEK293T cells

expressing *OsCNGC9^{S645A}* showed impaired cytosolic Ca^{2+} elevation compared with those expressing *OsCNGC9* (Figure 4G and 4H). These results indicate that the phosphorylation status of Ser645 positively regulates the calcium channel activity of OsCNGC9. Collectively, these data suggest that the phosphorylation of OsCNGC9 Ser645 by OsSAPK8 promotes cytosolic Ca^{2+} influx, thus enhancing chilling tolerance in rice.

OsSAPK8 positively regulates chilling tolerance and cold-induced Ca^{2+} influx in rice

To further test whether OsSAPK8 plays a role in the regulation of rice chilling tolerance, we conducted a chilling tolerance assay using two independent *OsSAPK8* knockout lines (Supplemental Figure 9). Consistent with a previous study (Zhong et al., 2020), the survival rate of the *OsSAPK8* knockout mutant plants was clearly lower than that of the corresponding WT (Nipponbare) seedlings after chilling treatment (Figure 5A and 5B; Supplemental Figure 2D). Interestingly, a Ca^{2+} flux assay showed that root cells of Nipponbare but not those of the *OsSAPK8* knockout mutants exhibited more significant Ca^{2+} influx after cold treatment (Figure 5C and 5D). In addition, a cytoplasmic Ca^{2+} assay showed that the *OsSAPK8* knockout mutants also exhibited lower [Ca^{2+}]$_{cyt}$ cold responses compared with Nipponbare (Figure 5E). qRT–PCR analysis showed that in response to chilling stimulation, the induction of cold stress-related gene expression was significantly lower in *OsSAPK8* knockout mutants than in Nipponbare (Figure 5F and 5G). These results collectively suggest that OsSAPK8 participates in the regulation of chilling tolerance and cold-induced Ca^{2+} influx in rice.

To evaluate the potential value of *OsSAPK8* in crop genetic improvement, we performed a chilling tolerance assay in the *OsSAPK8-GFP* overexpression line (Lin et al., 2015) and Nipponbare. qRT–PCR analysis confirmed the overexpression of *OsSAPK8* in *OsSAPK8-GFP* overexpression plants compared with Nipponbare (Supplemental Figure 12A). After chilling treatment and recovery, the survival rate of the *OsSAPK8-GFP* overexpression plants was greater than 60%, whereas that of Nipponbare plants was less than 30% under the same conditions (Supplemental Figures 2E, 12B, and 12C). An *in vivo* phosphorylation assay showed that the relative phosphorylation intensity of OsCNGC9-C was more strongly induced in the *OsSAPK8-GFP* overexpression plants than in Nipponbare after cold shock (Supplemental Figure 13A). In addition, a Ca^{2+} flux assay showed that in response to cold stimulation, root cells of the *OsSAPK8-GFP* overexpression plants exhibited stronger Ca^{2+} influx than those of Nipponbare (Supplemental Figure 13B and 13C). After cold shock, the *OsSAPK8-GFP* overexpression plants consistently showed higher levels of cold stress-related gene expression compared with Nipponbare (Supplemental Figure 13D and 13E), suggesting that OsSAPK8-mediated

(F) Survival rate of Kitaake, *OsCNGC9-OE*, and *OsCNGC9^{S645D}-OE* plants before and after cold treatment. Values are means ± SD (*n* = 6, six technical replicates per biological repeat and at least 18 seedlings per technical replicate; *P* < 0.05, **P* < 0.01, Student's *t*-test).
(G and H) Ca^{2+} imaging of the HEK293T cells showing the channel activity of OsCNGC9, OsCNGC9-C^{S645A}, and OsCNGC9^{S645D}. Average fluorescence intensity changes **(G)** and peak fluorescence intensity **(H)** in HEK293T cells transiently expressing various tested proteins as indicated. Values are means ± SD (*n* ≥ 30; *P* ≤ 0.05, Student's *t*-test). Significant differences are indicated by different lowercase letters.
All experiments except LC–MS/MS were repeated three times with similar results.
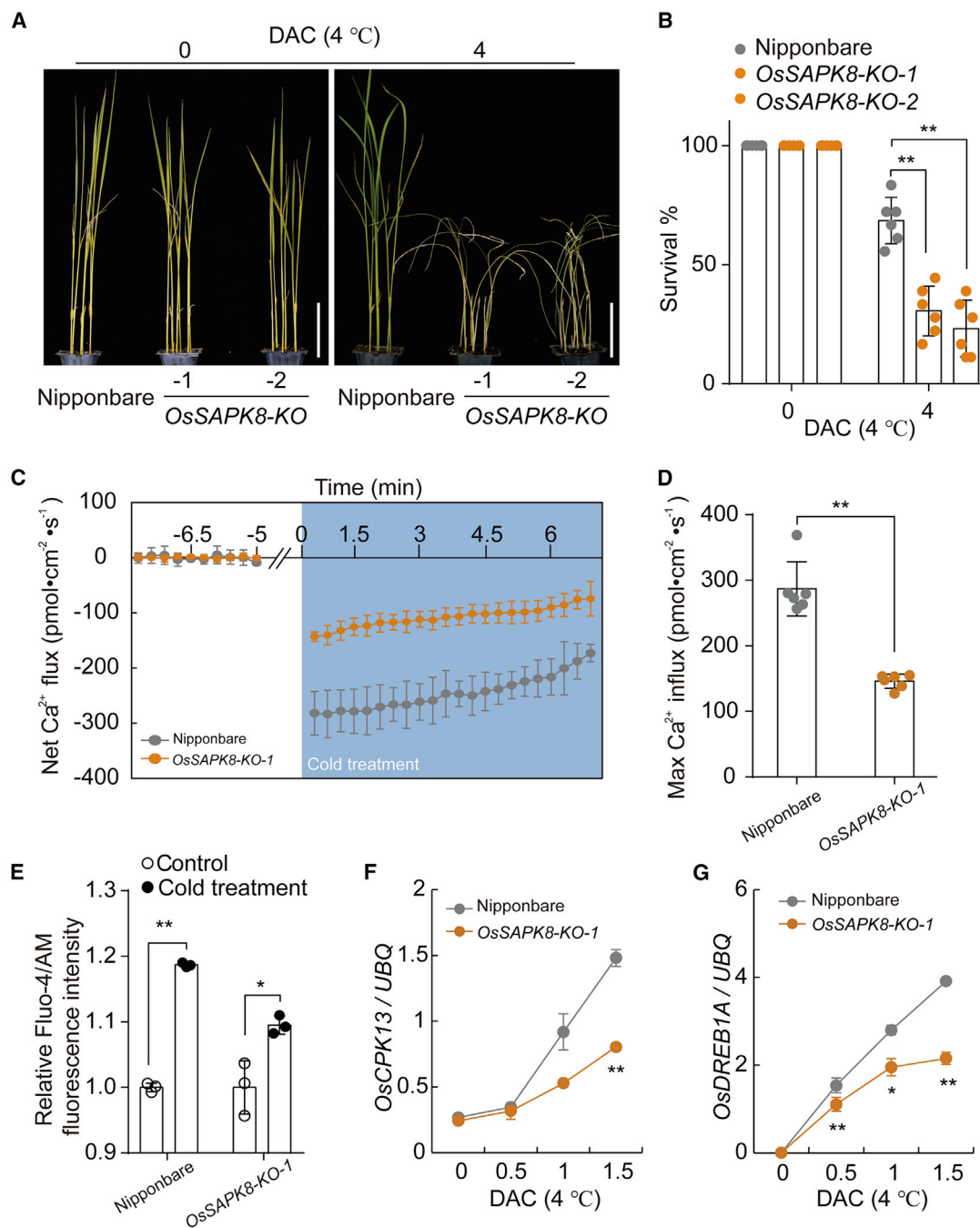
Figure 5. The *OsSAPK8* knockout mutants showed impaired chilling tolerance, cold-induced Ca²⁺ influx, and cold stress-related gene expression.

(A) Chilling tolerance phenotype of Nipponbare and the *OsSAPK8* knockout mutant plants. Seedlings were incubated at 4°C for the indicated days and then transferred back to the normal temperature for 7 days of recovery. DAC, days after cold treatment. Scale bars, 5 cm.

(B) Survival rates of Nipponbare and the *OsSAPK8* knockout mutant plants before and after cold treatment. Values are means ± SD ($n = 6$, six technical replicates per biological repeat and at least 18 seedlings per technical replicate; compared with Nipponbare, **$P < 0.01$, Student's *t-test*).

(C) Comparison of extracellular calcium influx in the living roots of Nipponbare and the *OsSAPK8* knockout plants upon cold shock. The blue background indicates the duration of cold treatment.

(D) Calculated maximum Ca²⁺ influxes from **(C)**. Values are means ± SD ($n = 6$; compared with Nipponbare, **$P < 0.01$, Student's *t-test*).

(E) Quantification of the Fluo-4/AM fluorescence intensity. Data were obtained from 20 000 protoplast cells using flow cytometry. The fluorescence intensity of the room temperature sample was defined as 1. Values are means ± SD ($n = 3$; *$P < 0.05$, **$P < 0.01$, Student's *t-test*).

(F and G) Dynamic change in the expression levels of the cold stress-related genes *OsCPK13* and *OsDREB1A* in Nipponbare and the *OsSAPK8* knockout mutant plants in response to cold stress. Values are means ± SD ($n = 3$; compared with Nipponbare, *$P < 0.05$, **$P < 0.01$, Student's *t-test*).

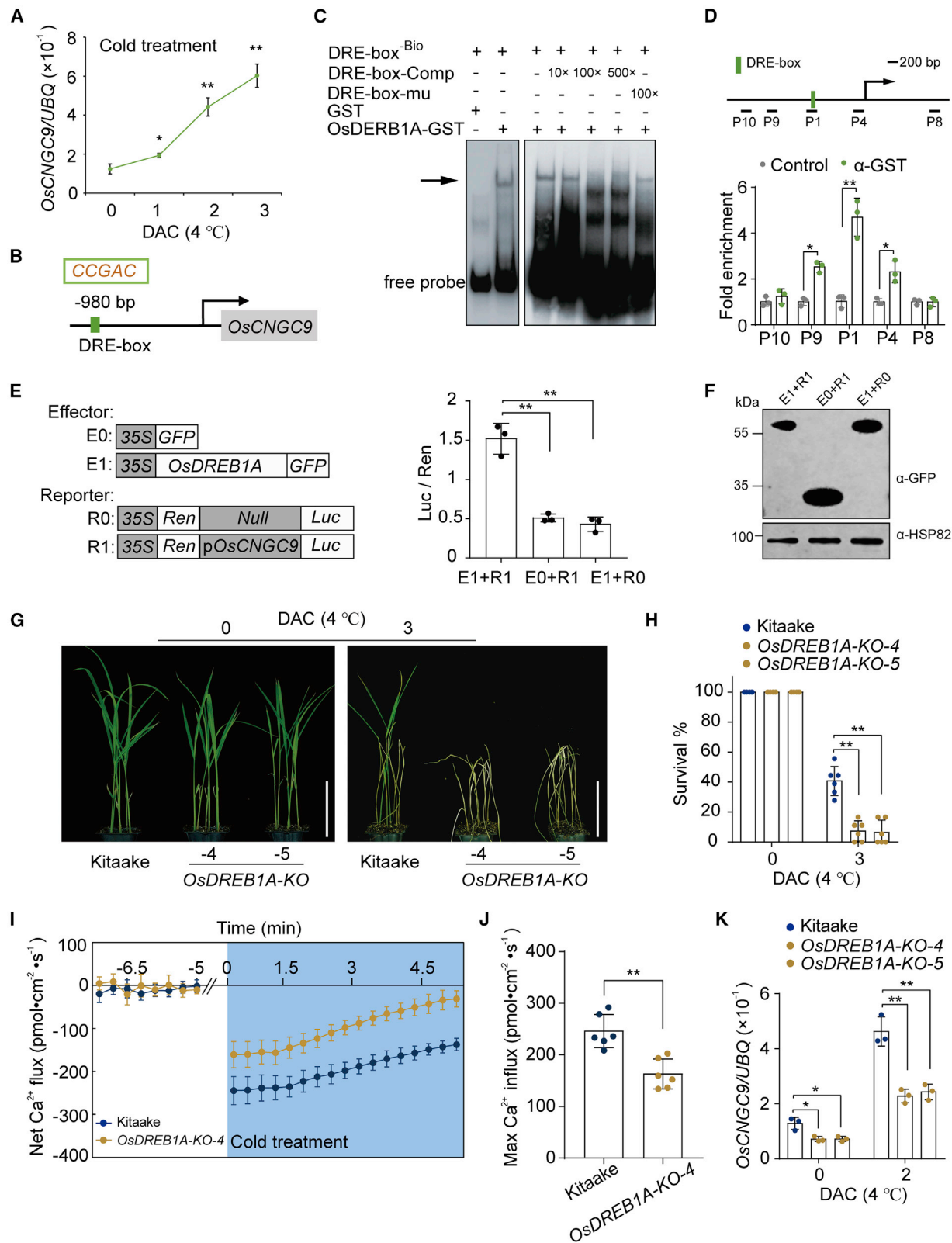All experiments were repeated at least three times with similar results.

Figure 6. OsDREB1A promotes *OsCNGC9* transcription by directly binding to the DRE-box motif in the *OsCNGC9* promoter.
(A) The transcript level of *OsCNGC9* can be induced by cold treatment. Values are means ± SD (*n* = 3; compared with the value at DAC 0, *P* < 0.05, **P* <
0.01, Student's *t-test*). DAC, days after cold treatment.
(B) Schematic diagram of the DRE-box (5′-CCGAC-3′) motif in the *OsCNGC9* promoter. DRE-box, a putative DREB-binding site.

phosphorylation of OsCNGC9 plays an important role in rice chilling tolerance.

OsDREB1A promotes *OsCNGC9* transcription by directly binding to the DRE-box motif in the *OsCNGC9* promoter

Consistent with a previous study (Nawaz et al., 2014), our qRT–PCR analysis showed that the transcription of *OsCNGC9* was significantly induced by chilling stress (Figure 6A). To obtain further insights into the regulatory mechanism of *OsCNGC9* at the transcriptional level, we analyzed the *OsCNGC9* promoter with PlantPAN 2.0 and identified one dehydration response element (*DRE/CRT*) that has been reported to participate in cold, drought, and salt stress responses (Figure 6B) (Yamaguchi-Shinozaki and Shinozaki, 1994; Chow et al., 2016). Previous studies have shown that OsDREB1A, a DRE-box motif-binding protein in rice, positively regulates cold tolerance by inducing stress-related gene expression (Dubouzet et al., 2003). Therefore, we investigated whether OsDREB1A directly regulates *OsCNGC9* transcription by binding to the DRE-box motif *in vitro* using a DNA electrophoretic mobility shift assay (EMSA). The OsDREB1A-GST fusion protein, but not the free GST (glutathione *S*-transferase) protein, was able to bind to the DNA probe containing the DRE-box element (Figure 6C). Moreover, a DRE-box probe without biotin labeling effectively competed for OsDREB1A binding with the DRE-box-containing probe. In addition, the OsDREB1A-GST fusion protein could not bind to DRE-box-mu, a mutant version of the DRE-box probe (Figure 6C). We further performed chromatin immunoprecipitation (ChIP)–qPCR to examine the ability of OsDREB1A to bind to different regions of the *OsCNGC9* promoter, and only the P1 fragment containing the DRE-box motif was significantly enriched (Figure 6D).

To further verify that *OsCNGC9* is a direct target of OsDREB1A, we conducted a transient transfection assay in rice protoplasts. We observed a positive effect of OsDREB1A on the expression level of the *LUC* reporter gene driven by the *OsCNGC9* promoter (Figure 6E and 6F). We also conducted a chilling tolerance assay using two independent *OsDREB1A* knockout lines (*OsDREB1A-KO*; Supplemental Figure 14). Consistent with previous reports, the loss of *OsDREB1A* function increased susceptibility to

chilling stress compared with the WT, Kitaake (Figure 6G and 6H; Supplemental Figure 2F). In addition, a Ca^{2+} flux assay showed that the *OsDREB1A-KO* plants exhibited weaker extracellular Ca^{2+} influx compared with Kitaake in response to cold stress (Figure 6I and 6J). Consistently, qRT–PCR analysis showed that the transcript level of *OsCNGC9* was induced to a lesser extent in the *OsDREB1A-KO* plants compared with Kitaake in response to chilling stimulation (Figure 6K). Taken together, these results indicate that chilling stimulation promotes *OsCNGC9* expression through an OsDREB1A-dependent pathway.

DISCUSSION

Although calcium channels have been implicated as key components in cold signal transduction, the long-sought-after calcium channels responsible for cold stress signaling pathways in plants have remained elusive. In this study, we present several lines of evidence to support the notion that OsCNGC9 acts as a calcium channel required for chilling tolerance. First, we showed that the *cds1* knockout mutant is hypersensitive to chilling, whereas *OsCNGC9* overexpression plants exhibit significantly enhanced chilling tolerance (Figure 1 and Supplemental Figure 6). Second, we demonstrated that OsCNGC9, a Ca^{2+}-permeable divalent cation-selective inward channel, is required for extracellular Ca^{2+} influx, $[Ca^{2+}]_{cyt}$ elevation, and cold stress-related gene expression in response to cold stress in rice (Figure 2 and Supplemental Figure 4). Third, we used multiple assays to show that elevated *OsCNGC9* level is important for cold shock-dependent changes in Ca^{2+} influx (Supplemental Figure 7). In addition, we found that a SnRK2 kinase, OsSAPK8, interacts with and phosphorylates OsCNGC9 at Ser645 to enhance its channel activity under cold stress, resulting in $[Ca^{2+}]_{cyt}$ elevation and enhanced chilling tolerance in rice (Figures 3 and 4). Consistently, we showed that OsSAPK8 also functions as a positive regulator of cold tolerance and extracellular Ca^{2+} influx upon cold shock (Figure 5; Supplemental Figures 12 and 13). Furthermore, we demonstrated that the expression of *OsCNGC9* can be directly activated by OsDREB1A in response to chilling stimulation and that the knockout of *OsDREB1A* causes impaired cold tolerance, weaker cold-induced Ca^{2+} influx, and lower *OsCNGC9* expression compared with Kitaake (Figure 6).

(C) An EMSA assay shows that OsDREB1A directly binds to the DRE-box motif in the *OsCNGC9* promoter. Arrow indicates the shifted band representing the protein–DNA complex. The plus (+) and minus (−) signs denote the presence or absence of the protein in each sample.

(D) An *in vitro* ChIP–qPCR assay showed that OsDREB1A binds to the *OsCNGC9* promoter. The DRE-box motif is located 980 bp upstream of the start codon of *OsCNGC9*. Black horizontal lines show the amplified regions of qRT–PCR analysis. The fold enrichment was normalized against the rice *UBIQUITIN* promoter. Values are means ± SD ($n = 3$; *$P < 0.05$, **$P < 0.01$, Student's *t-test*).

(E and F) An *in vivo* split-luciferase assay verified the binding of OsDREB1A to the *OsCNGC9* promoter region in rice protoplasts. Various constructs used in the luciferase assay are shown on the left of the histogram. Immunoblots show the levels of protein accumulation **(F)**. Values are means ± SD ($n = 3$; **$P < 0.01$, Student's *t-test*).

(G) Chilling tolerance phenotype of Kitaake and the *OsDREB1A* knockout plants. Seedlings were incubated at 4°C for the indicated days and then transferred back to normal temperature for recovery. DAC, days after cold treatment. Scale bars, 5 cm.

(H) Survival rate of Kitaake and the *OsDREB1A* knockout plants before and after cold treatment. Values are means ± SD ($n = 6$, six technical replicates per biological repeat and at least 18 seedlings per technical replicate; **$P < 0.01$, Student's *t-test*).

(I) Comparison of extracellular calcium influx in the living roots of Kitaake and the *OsDREB1A-KO* plants upon cold shock. The blue background indicates the duration of cold treatment.

(J) Calculated maximum Ca^{2+} influxes from **(I)**. Values are means ± SD ($n = 6$; compared with Kitaake, **$P < 0.01$, Student's *t-test*).

(K) Expression level of *OsCNGC9* in Kitaake and the *OsDREB1A* knockout plants before and after cold treatment. Values are means ± SD ($n = 3$; compared with Kitaake, *$P < 0.05$, **$P < 0.01$, Student's *t-test*).

All experiments except **(B)** were repeated three times with similar results.
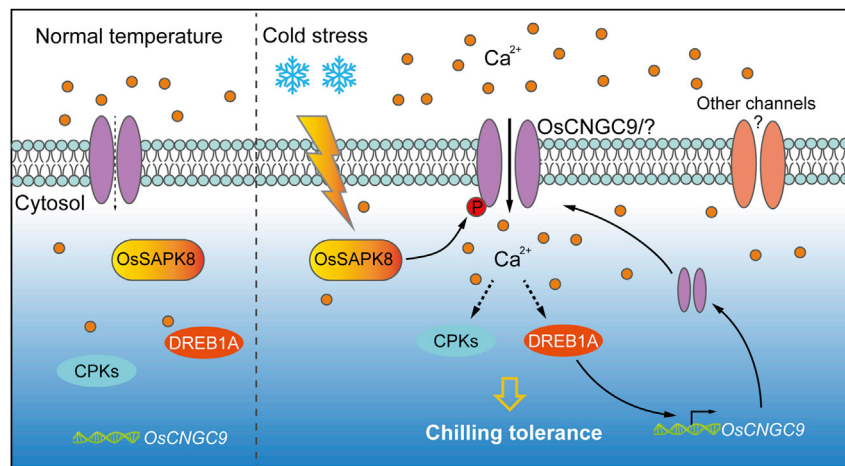
Figure 7. Proposed working model depicting the roles of OsCNGC9 in cold stress signaling.

OsSAPK8, a homolog of *Arabidopsis* OST1, is inactive under normal temperature conditions, and the channel activity of OsCNGC9 is relatively low to maintain a resting $[Ca^{2+}]_{cyt}$ level. In response to cold stress, OsSAPK8 phosphorylates and activates OsCNGC9, triggering Ca^{2+} influx and the activation of cold stress-related genes (e.g., *CPKs* and *Os-DREB1A*). OsDREB1A in turn promotes *OsCNGC9* transcription by directly binding to the DRE-box motif in the *OsCNGC9* promoter. Thus, OsSAPK8-mediated OsCNGC9 phosphorylation and OsDREB1A-mediated *OsCNGC9* expression form a potential positive feedback loop, leading to enhanced OsCNGC9-mediated Ca^{2+} influx and chilling tolerance in rice. "OsCNGC9/?" represents the potential homomeric and/or heteromeric tetramers that contain OsCNGC9.

Based on the data collected above, we propose a working model of rice cold stress response in which OsSAPK8 phosphorylates and activates OsCNGC9, triggering Ca^{2+} influx and the activation of cold stress-related genes. In addition, the expression of *OsCNGC9* is enhanced by OsDREB1A, leading to enhanced OsCNGC9-mediated Ca^{2+} influx and chilling tolerance in rice (Figure 7). Our model is consistent with earlier reports that OsSAPK8 functions as a positive regulator of responses to abiotic stresses, including cold stress (Zhong et al., 2020), and that *Arabidopsis* OST1, a homolog of rice OsSAPK8, positively regulates cold tolerance by phosphorylating critical regulators upstream of CBFs (Ding et al., 2015, 2018, 2019). Together with these previous findings, our results suggest that a conserved regulatory mechanism composed of SnRKs-CNGCs may regulate cold-triggered cytoplasmic calcium elevation and chilling tolerance in both monocots and dicots.

A recent study showed that COLD1 works together with RGA1 to activate the Ca^{2+} channel and then mediates cold-induced Ca^{2+} influx to promote cold stress tolerance in rice. However, it remains unclear whether COLD1 functions as a Ca^{2+}-permeable channel or a subunit of the Ca^{2+} channel in this process (Ma et al., 2015; Manishankar and Kudla, 2015). In the future, it will be interesting to study whether OsCNGC9 functions cooperatively with COLD1 in chilling tolerance.

In this study, we showed that OsSAPK8 phosphorylates the C terminus of OsCNGC9 to enhance its channel activity upon cold stress and that Ser645 is a major phosphorylation site for OsSAPK8 in response to cold stress (Figures 3 and 4). It is notable that the Ser645A mutation only partially abolishes OsSAPK8-mediated or cold stress-induced phosphorylation of OsCNGC9-C (Figure 4B and 4C), indicating that other putative phosphorylation sites at the C terminus of OsCNGC9 may also contribute to OsSAPK8-mediated OsCNGC9 activation in response to chilling stress. This notion is consistent with reports that the C terminus of mammalian CNGCs is important for subunit interactions and channel activity (Lee and MacKinnon, 2017) and that multiple phosphorylation sites in the CNGC protein are involved in the regulation of innate immunity and cell death in *Arabidopsis* (Tian et al., 2019; Yu et al., 2019). The physiological

role of these additional phosphorylation sites remains to be characterized in the future.

Earlier studies have documented that the activity of CNGCs can be regulated by calmodulin (CaM) and 3',5'-cyclic nucleotide monophosphate (cNMP) (DeFalco et al., 2016b; Pan et al., 2019; Tian et al., 2019). For example, it has been reported that active AtBIK1 phosphorylates and activates the CaM-gated AtCNGC2–AtCNGC4 channel to trigger Ca^{2+} influx and enhance defense against plant pathogens (Tian et al., 2019), indicating that AtBIK1 may relieve the inhibition of CaM on CNGC channel activity in plant cells. Interestingly, the C-terminal cytosolic part of OsCNGC9 contains a potential CaM-binding domain (CaMBD) and a potential cyclic nucleotide-binding domain, suggesting that OsCNGC9 may also be regulated by OsCaMs or cNMP (Supplemental Figure 11). This possibility awaits further testing.

We previously reported that the *cds1* mutant shows reduced pathogen resistance at the seedling stage and a lesion-mimic phenotype after flowering (Wang et al., 2019). Interestingly, the *Arabidopsis cpr22* mutant (a gain-of-function mutant of CNGCs) also displays a lesion-mimic phenotype, and its programmed cell death (PCD) phenotype is temperature sensitive (Yoshioka et al., 2001; Mosher et al., 2010). Low temperature (16°C) enhances the *cpr22* mutant's PCD phenotype, and like *cds1*, this mutant will die under 4°C treatment (Chin et al., 2010; Mosher et al., 2010). The null mutants for *CNGC2* (*dnd1*) and *CNGC4* (*dnd2*) also show temperature-sensitive and autoimmune phenotypes (Yu et al., 1998; Jurkowski et al., 2004; Finka et al., 2012). Moreover, both *Arabidopsis CNGC2* and its putative moss ortholog *PpCNGCb* have been shown to play a critical role in thermotolerance (Finka et al., 2012). Whether and how the temperature regulation of OsCNGC9 channel activity is related to the lesion-mimic phenotype of the *cds1* mutant remains unknown. It is worth noting that tobacco mosaic virus resistance conferred by the *N* gene is temperature sensitive (Takabatake et al., 2006). Another recent study showed that the lesion-mimic phenotype of *bak1* is dependent on *ADR1*s, a group of *NLR*s (Wu et al., 2020). Because the *cds1* mutant has no lesion-mimic phenotype at the seedling stage,

we speculated that an unknown developmental stage-dependent activation of NLR (nucleotide-binding domain leucine-rich repeat containing protein) may be involved in triggering the autoimmunity phenotype of *cds1* after flowering (Wang et al., 2019), a hypothesis that remains to be tested in future studies.

Low environmental temperature negatively affects crop growth and development. Therefore, chilling tolerance is one of the most critical traits to consider in crop genetic improvement (Zhang et al., 2019). Our results show that the precise regulation of *OsCNGC9* and *OsSAPK8* can improve chilling tolerance in rice (Figure 4; Supplemental Figures 6 and 12), thus providing a useful strategy for the improvement of chilling tolerance in rice.

METHODS

Plant materials and growth conditions

The *cds1* mutant, as well as *OsCNGC9* complementation (*pGOsCNGC9*), *OsCNGC9* overexpression (*OsCNGC9-OE*), and *OsSAPK8* overexpression (*OsSAPK8-GFP*) lines, were described previously (Lin et al., 2015; Wang et al., 2019). The *OsSAPK8* and *OsDREB1A* knockout lines and *OsCNGC9^{S645D}-OE* transgenic lines were generated using *Agrobacterium*-mediated transformation. All plants were grown in a greenhouse or a controlled growth chamber at the Chinese Academy of Agricultural Sciences (Beijing) for phenotypic analyses.

Evaluation of chilling and heat tolerance

Cold treatments were performed as described previously with minor modifications (Ma et al., 2015). In brief, rice seedlings were grown in a controlled growth chamber (12 h light at 30°C/12 h darkness at 28°C, relative humidity of ~70%, and light intensity of ~800 μmol m^{-2} s^{-1}) for about 2 weeks, then exposed to chilling treatment (4°C) or heat treatment (45°C) under the same photoperiod conditions. The evaluation of chilling tolerance or heat tolerance based on survival rate was measured after chilling or heat treatment for the indicated number of days and 7 days of recovery.

Ca^{2+} flux assay with non-invasive micro-test technology

Net Ca^{2+} flux was measured using NMT (NMT-YG-100; Younger USA, Amherst, MA, USA) as previously described with minor modifications (Ma et al., 2015). Roots sampled from rice seedlings were immobilized in the measuring buffer (0.1 mM KCl, 0.1 mM CaCl$_2$, 0.1 mM MgCl$_2$, 0.5 mM NaCl, 0.3 mM 2-(*N*-morpholino)ethanesulfonic acid [MES], and 0.2 mM Na$_2$SO$_4$; pH 6.0) for 30 min of equilibration, and the steady-state fluxes in rice root cells were then continuously recorded for the indicated times at room temperature prior to cold treatments. To avoid the adverse effects of system operation, data recording was stopped during the preparation for cold treatment. During this period, the samples were kept at normal temperature. Cold treatment was carried out by replacing the room-temperature test buffer with ice-cold test buffer. Ice-cold test buffer was added quickly to the container around the roots, and the transient flux of Ca^{2+} was recorded. Ca^{2+} flux was examined in a zone about 500 μm from the root tip. All measurement results were imported and converted into net Ca^{2+} flux using JCal v3.3 (a free Microsoft Excel spreadsheet available from youngerusa.com or xbi.org).

Measurement of [Ca^{2+}]$_{cyt}$ with YC3.6 and Fluo-4 AM

For YC3.6 fluorescence observation, the WT, *cds1*, and *PGOsCNGC9* were each crossed with *UBQ10::YC3.6* transgenic plants (Behera et al., 2015). Roots of the WT, homozygous mutants, and *PGOsCNGC9*-containing mutants from F2 populations were excised with a razor. The roots of 5-day-old rice seedlings were fixed to the bottom of a glass dish with medical fabric. To maintain moisture, 250 μl of half-strength Murashige and Skoog (1/2 MS) buffer was added to the roots

in the dish. For cold shock, 3 ml of ice-cold 1/2 MS buffer was added to the glass dish without interrupting image acquisition. YC3.6 fluorescence was examined in a zone about 500 μm from the root tip cell at the single-cell level. Ca^{2+} imaging was performed directly on a confocal laser scanning microscope (Zeiss LSM980) at 458 nm (excitation) and 525 nm (detection). The imaging parameters were as follows: image dimension (256 × 256), pinhole (1 airy unit), and line sequential. Images were acquired every 2 s, and a ZEN microscope and imaging software were used to monitor the mean fluorescence intensity. The mean fluorescence intensity at CFP and YFP channels was recorded, and the YFP/CFP ratio was calculated. The [Ca^{2+}]$_{cyt}$ level was directly indicated by the YFP/CFP ratio, as described previously (Krebs et al., 2012).

For Fluo-4 AM staining, rice protoplasts were prepared as described previously (Zhang et al., 2011). In brief, 0.5- to 1-mm strips from leaves of rice seedlings were digested in an enzyme solution containing 1.5% cellulose and 0.3% macerozyme in darkness. The strips were incubated in the enzyme solution for about 4 h in the dark with gentle shaking (40 rpm) at room temperature (28°C). The enzyme solution was then removed and W5 medium (154 mM NaCl, 125 mM CaCl$_2$, 5 mM KCl, and 2 mM MES; pH 5.7) was added. Next, the W5 medium containing the protoplasts was transferred and the protoplasts filtered through a 35-μm nylon mesh. The W5 medium was carefully removed after centrifugation. The protoplasts were resuspended with SM solution (0.4 M mannitol, 20 mM CaCl$_2$, and 5 mM MES; pH 5.7). For Fluo-4 AM staining, 5 mM Fluo-4 AM and 0.02% Pluronic F-127 (Beijing Solarbio Science & Technology) were added to the suspension buffer containing the protoplasts and incubated at 37°C for 1 h (Hillson and Hallett, 2007). The samples were placed on ice for 1 min for cold treatment. Fluorescence intensity was measured using a flow cytometer (MoFlo XDP; Beckman Coulter, USA). Fluo-4 AM-labeled cells out of 20 000 were selected and detected. Fluorescence from the protoplasts loaded with Fluo-4/AM was also detected using a laser scanning confocal microscope (Zeiss LSM 700) at 488 nm (excitation) and 520 nm (detection).

Plasmid construction and plant transformation

To generate CRISPR/Cas9 constructs, an 18-bp gene-specific sequence of *OsSAPK8* or *OsDREB1A* was synthesized and annealed to form an oligo adaptor. The oligo adaptors were then cloned into the pOs-Cas9 vector to generate CRISPR/Cas9 constructs (Miao et al., 2013). The CRISPR/Cas9 plasmids were introduced into rice using *Agrobacterium*-mediated transformation. Positive lines were confirmed by PCR followed by sequencing. Stable T2 or T3 transgenic progenies were analyzed. All primer sequences used here and in the following sections are listed in Supplemental Table 4.

RNA isolation and qRT–PCR assays

Total RNA isolation and qRT–PCR assays were performed as previously described (Wang et al., 2016). In brief, total RNA was extracted from rice tissues using an RNeasy Plant Mini Kit (Zymo). Reverse transcription was performed using a QuantiTect Reverse Transcription Kit (Qiagen), and qRT–PCR was performed using a SYBR Premix Ex Taq Kit (TaKaRa) and an ABI Prism 7500 Real-Time PCR System.

Electrophoretic mobility shift assay

The electrophoretic mobility shift assay was carried out using the Light-Shift Chemiluminescent EMSA Kit (Thermo Fisher) according to the manufacturer's instructions. Recombinant OsDREB1A-GST fusion proteins were purified using BeaverBeads GSH (Beaver) after incubation. Biotin-labeled DNA probes were synthesized by Invitrogen (Shanghai, China). Photos were obtained with a charge-coupled device camera.

In vitro ChIP assay

The ChIP assay was performed as described previously (Li et al., 2017). Total DNA was extracted from 1-month-old Kitaake rice plants and sheared into fragments of 100–500 bp. The DNA fragments and

OsDREB1A-GST fusion protein were co-incubated in an incubation buffer for 2 h. After washing and breaking down, the DNA fragments were extracted for ChIP–qPCR.

Luciferase reporter assay

The luciferase reporter assay was performed as described previously (Duan et al., 2019). To generate the effector construct, we cloned the full-length coding sequence of *OsDREB1A* into the pAN580 vector. To generate the reporter construct, we cloned the promoter region of *OsCNGC9* into the pGreenII vector. Effector and reporter plasmids were then co-transformed into rice protoplasts for the luciferase activity assay. Luciferase activity was measured using the Dual-Luciferase reporter assay system (E1910; Promega).

Yeast two-hybrid assay

A Y2H assay was used to detect protein interactions using the DUAL-hunter system (Dualsystems Biotech). The indicated sequences were fused to the Cub fragment in the pXGY17 vector or to the Nub fragment in the pXGY18 vector. The Y2H assay was conducted according to a method described previously (Xu et al., 2017).

Luciferase complementation assay

The luciferase complementation assay was conducted as described previously (Chen et al., 2008). *Agrobacterium* cells harboring the nLUC and cLUC constructs were co-infiltrated into *N. benthamiana* leaves. Leaves were harvested 2 days later and incubated with 1 mM luciferin, and luminescence activity was recorded with the NightSHADE LB 985 system (Berthold). The interactions with GW5 were used as negative controls, and the interaction between OsCNGC9 and OsRLCK185 was used as the positive control (Liu et al., 2017; Wang et al., 2019).

Co-immunoprecipitation assays in rice protoplasts

To verify the *in vivo* interaction between OsCNGC9 and OsSAPK8, we performed co-immunoprecipitation assays as described previously (Wang et al., 2019). Rice protoplasts were transfected with the indicated plasmids and incubated overnight. Total protein was extracted with 10 ml of ice-cold IP buffer (150 mM KCl, 50 mM HEPES [pH 7.5], 1 mM dithiothreitol [DTT], 0.4% Triton-X 100, and proteinase inhibitor cocktail). Debris was removed from the lysate by centrifugation at 12 000 g for 30 min. Supernatants of 100 μl were stored as input samples, and the remaining supernatant was incubated with GFP-Trap magnetic beads (ChromoTek). Western blots were conducted with anti-GFP (Roche 11814460001, dilution 1:3000) and anti-FLAG (MBL M185-7, dilution 1:3000) antibodies.

In vitro phosphorylation assay

The *in vitro* phosphorylation assay was performed as previously described with slight modifications (Wang et al., 2019). In brief, the HIS-OsSAPK8 recombinant protein was expressed in *Escherichia coli* strain BL21, and the OsCNGC9-C-FLAG, OsCNGC9-C^{S645A}-FLAG, or OsCNGC9-C^{5A}-FLAG recombinant protein was expressed in rice protoplasts. Phosphorylation assays were performed with purified beads containing HIS-OsSAPK8 and different versions of OsCNGC9-C-FLAG in 30 μl of kinase buffer (40 mM HEPES [pH 7.5], 20 mM MgCl$_2$, 1 mM DTT, 2 mM ATP, proteinase inhibitor cocktail, and phosphatase inhibitor cocktail) for 90 min at 30°C, and the reaction was stopped by adding SDS loading buffer. Different versions of OsCNGC9-C-FLAG phosphorylation were detected by the Phos-tag assay with an anti-FLAG antibody (MBL M185-7, dilution 1:3000).

In vivo phosphorylation assay

The *in vivo* phosphorylation assay was carried out as described previously (Bi et al., 2018). Rice protoplasts were transfected with the indicated plasmids and treated with cold stress, and proteins were extracted using IP buffer without EDTA. The samples were subsequently analyzed using 10% SDS–polyacrylamide gels with or without 100 μM MnCl$_2$ and 75 μM Phos-tag acrylamide AAL-107 (NARD Institute). For Phos-tag

SDS–PAGE, after electrophoresis the gel was incubated in transfer buffer containing 1 mM EDTA three times for 20 min each, followed by incubation in transfer buffer without EDTA three times. The samples were then transferred to polyvinylidene fluoride membranes, followed by immunoblot analysis with anti-FLAG (MBL M185-7, dilution 1:3000) and anti-HSP82 (Beijing Protein Innovation AbM51099-31-PU, dilution 1:3000) antibodies.

Calcium imaging assay

Changes in intracellular Ca^{2+} were assessed in HEK293T cells as described previously with minor modifications (Wang et al., 2019). Prior to Ca^{2+} imaging, HEK293T cells were transfected with the indicated plasmids and cultured in a CO$_2$ incubator at 37°C for 2 days. YC3.6 fluorescence was recorded using an inverted microscope (D1; Carl Zeiss, Germany) by monitoring the ratio (535 nm/480 nm) of YC3.6. Data acquisition and analysis were carried out using MAG Biosystems 7.5 software (MetaMorph, USA). For each experiment, images were acquired every 4 s and the field was recorded for about 7 min. The standard external working solution (120 mM NaCl, 10 mM HEPES, 10 mM glucose, 3 mM KCl, 1.2 mM NaHCO$_3$, and 1 mM MgCl$_2$; pH 7.2) was used for the Ca^{2+} imaging assay. External Ca^{2+} was added to the standard external working solution as indicated.

SUPPLEMENTAL INFORMATION

Supplemental Information is available at *Molecular Plant Online*.

AUTHOR CONTRIBUTIONS

J. Wan and H.W. supervised the project. J. Wang, Y.R., and Xi Liu designed the research. J. Wang performed most of the experiments. Xi Liu provided the *cds1* mutant. S.L., Xiao Zhang, Xin Liu, Y.Z., B.L., and C.Z. performed the cold tolerance assay. T.P., Yongfei Wang, M.W., and R.J. performed the luciferase complementation assay. Xin Zhang, X.G., L.J., Y.W., Z.C., Q.L., C.L., F.W., S.Z., Y.X., M.H., Y.Y., X. Zheng, Z.Z., and Yong-Fei Wang provided technological assistance. J. Wang and Y.R. analyzed the data and wrote the manuscript. J. Wan and H.W. revised the manuscript. J. Wang, Y.R., and Xi Liu contributed equally to this work.

REFERENCES

Barrero-Gil, J., and Salinas, J. (2013). Post-translational regulation of cold acclimation response. Plant Sci. **205-206**:48–54.

Behera, S., Wang, N., Zhang, C., Schmitz-Thom, I., Strohkamp, S., Schultke, S., Hashimoto, K., Xiong, L., and Kudla, J. (2015). Analyses of Ca²⁺ dynamics using a ubiquitin-10 promoter-driven Yellow Cameleon 3.6 indicator reveal reliable transgene expression and differences in cytoplasmic Ca²⁺ responses in *Arabidopsis* and rice (*Oryza sativa*) roots. New Phytol. **206**:751–760.

Bi, G., Zhou, Z., Wang, W., Li, L., Rao, S., Wu, Y., Zhang, X., Menke, F.L.H., Chen, S., and Zhou, J.M. (2018). Receptor-like cytoplasmic kinases directly link diverse pattern recognition receptors to the activation of mitogen-activated protein kinase cascades in *Arabidopsis*. Plant Cell **30**:1543–1561.

Carpaneto, A., Ivashikina, N., Levchenko, V., Krol, E., Jeworutzki, E., Zhu, J.K., and Hedrich, R. (2007). Cold transiently activates calcium-permeable channels in *Arabidopsis* mesophyll cells. Plant Physiol. **143**:487–494.

Chen, H., Zou, Y., Shang, Y., Lin, H., Wang, Y., Cai, R., Tang, X., and Zhou, J.M. (2008). Firefly luciferase complementation imaging assay for protein-protein interactions in plants. Plant Physiol. **146**:368–376.

Chin, K., Moeder, W., Abdel-Hamid, H., Shahinas, D., Gupta, D., and Yoshioka, K. (2010). Importance of the αC-helix in the cyclic nucleotide binding domain for the stable channel regulation and function of cyclic nucleotide gated ion channels in *Arabidopsis*. J. Exp. Bot. **61**:2383–2393.

Chow, C.N., Zheng, H.Q., Wu, N.Y., Chien, C.H., Huang, H.D., Lee, T.Y., Chiang-Hsieh, Y.F., Hou, P.F., Yang, T.Y., and Chang, W.C. (2016). PlantPAN 2.0: an update of plant promoter analysis navigator for reconstructing transcriptional regulatory networks in plants. Nucleic Acids Res. **44**:D1154–D1160.

DeFalco, T.A., Moeder, W., and Yoshioka, K. (2016a). Opening the gates: insights into cyclic nucleotide-gated channel-mediated signaling. Trends Plant Sci. **21**:903–906.

DeFalco, T.A., Marshall, C.B., Munro, K., Kang, H.G., Moeder, W., Ikura, M., Snedden, W.A., and Yoshioka, K. (2016b). Multiple calmodulin-binding sites positively and negatively regulate *Arabidopsis* CYCLIC NUCLEOTIDE-GATED CHANNEL12. Plant Cell **28**:1738–1751.

Ding, Y., Shi, Y., and Yang, S. (2019). Advances and challenges in uncovering cold tolerance regulatory mechanisms in plants. New Phytol. **222**:1690–1704.

Ding, Y., Li, H., Zhang, X., Xie, Q., Gong, Z., and Yang, S. (2015). OST1 kinase modulates freezing tolerance by enhancing ICE1 stability in *Arabidopsis*. Dev. Cell **32**:278–289.

Ding, Y., Jia, Y., Shi, Y., Zhang, X., Song, C., Gong, Z., and Yang, S. (2018). OST1-mediated BTF3L phosphorylation positively regulates CBFs during plant cold responses. EMBO J. **37**:e98228.

Duan, E., Wang, Y., Li, X., Lin, Q., Zhang, T., Wang, Y., Zhou, C., Zhang, H., Jiang, L., Wang, J., et al. (2019). OsSHI1 regulates plant architecture through modulating the transcriptional activity of IPA1 in rice. Plant Cell **31**:1026–1042.

Dubouzet, J.G., Sakuma, Y., Ito, Y., Kasuga, M., Dubouzet, E.G., Miura, S., Seki, M., Shinozaki, K., and Yamaguchi-Shinozaki, K. (2003). *OsDREB* genes in rice, *Oryza sativa* L., encode transcription activators that function in drought-, high-salt- and cold-responsive gene expression. Plant J. **33**:751–763.

Finka, A., Cuendet, A.F., Maathuis, F.J., Saidi, Y., and Goloubinoff, P. (2012). Plasma membrane cyclic nucleotide gated calcium channels control land plant thermal sensing and acquired thermotolerance. Plant Cell **24**:3333–3348.

Gao, F., Han, X., Wu, J., Zheng, S., Shang, Z., Sun, D., Zhou, R., and Li, B. (2012). A heat-activated calcium-permeable channel—*Arabidopsis* cyclic nucleotide-gated ion channel 6—is involved in heat shock responses. Plant J. **70**:1056–1069.

Guo, X., Liu, D., and Chong, K. (2018). Cold signaling in plants: insights into mechanisms and regulation. J. Integr. Plant Biol. **60**:745–756.

He, Y., Zhou, J., and Meng, X. (2019). Phosphoregulation of Ca²⁺ influx in plant immunity. Trends Plant Sci. **24**:1067–1069.

Hillson, E.J., and Hallett, M.B. (2007). Localised and rapid Ca²⁺ micro-events in human neutrophils: conventional Ca²⁺ puffs and global waves without peripheral-restriction or wave cycling. Cell Calcium **41**:525–536.

Jaglo-Ottosen, K.R., Gilmour, S.J., Zarka, D.G., Schabenberger, O., and Thomashow, M.F. (1998). *Arabidopsis CBF1* overexpression induces *COR* genes and enhances freezing tolerance. Science **280**:104–106.

Jurkowski, G.I., Smith, R.K., Jr., Yu, I.C., Ham, J.H., Sharma, S.B., Klessig, D.F., Fengler, K.A., and Bent, A.F. (2004). *Arabidopsis* DND2, a second cyclic nucleotide-gated ion channel gene for which mutation causes the "defense, no death" phenotype. Mol. Plant Microbe Interact. **17**:511–520.

Knight, H., Trewavas, A.J., and Knight, M.R. (1996). Cold calcium signaling in *Arabidopsis* involves two cellular pools and a change in calcium signature after acclimation. Plant Cell **8**:489–503.

Kobayashi, Y., Yamamoto, S., Minami, H., Kagaya, Y., and Hattori, T. (2004). Differential activation of the rice sucrose nonfermenting1-related protein kinase2 family by hyperosmotic stress and abscisic acid. Plant Cell **16**:1163–1177.

Kobayashi, Y., Murata, M., Minami, H., Yamamoto, S., Kagaya, Y., Hobo, T., Yamamoto, A., and Hattori, T. (2005). Abscisic acid-activated SNRK2 protein kinases function in the gene-regulation pathway of ABA signal transduction by phosphorylating ABA response element-binding factors. Plant J. **44**:939–949.

Krebs, M., Held, K., Binder, A., Hashimoto, K., Den Herder, G., Parniske, M., Kudla, J., and Schumacher, K. (2012). FRET-based genetically encoded sensors allow high-resolution live cell imaging of Ca²⁺ dynamics. Plant J. **69**:181–192.

Lee, C.H., and MacKinnon, R. (2017). Structures of the human HCN1 hyperpolarization-activated channel. Cell **168**:111–120.

Lesk, C., Rowhani, P., and Ramankutty, N. (2016). Influence of extreme weather disasters on global crop production. Nature **529**:84–87.

Li, W., Zhu, Z., Chern, M., Yin, J., Yang, C., Ran, L., Cheng, M., He, M., Wang, K., Wang, J., et al. (2017). A natural allele of a transcription factor in rice confers broad-spectrum blast resistance. Cell **170**:114–126.

Lin, Q., Wu, F., Sheng, P., Zhang, Z., Zhang, X., Guo, X., Wang, J., Cheng, Z., Wang, J., Wang, H., et al. (2015). The SnRK2-APC/C(TE) regulatory module mediates the antagonistic action of gibberellic acid and abscisic acid pathways. Nat. Commun. **6**:7981.

Liu, J., Chen, J., Zheng, X., Wu, F., Lin, Q., Heng, Y., Tian, P., Cheng, Z., Yu, X., Zhou, K., et al. (2017). *GW5* acts in the brassinosteroid signalling pathway to regulate grain width and weight in rice. Nat. Plants **3**:17043.

Liu, Q., Kasuga, M., Sakuma, Y., Abe, H., Miura, S., Yamaguchi-Shinozaki, K., and Shinozaki, K. (1998). Two transcription factors, DREB1 and DREB2, with an EREBP/AP2 DNA binding domain separate two cellular signal transduction pathways in drought- and low-temperature-responsive gene expression, respectively, in *Arabidopsis*. Plant Cell **10**:1391–1406.

Ma, Y., Dai, X., Xu, Y., Luo, W., Zheng, X., Zeng, D., Pan, Y., Lin, X., Liu, H., Zhang, D., et al. (2015). *COLD1* confers chilling tolerance in rice. Cell **160**:1209–1221.

Manishankar, P., and Kudla, J. (2015). Cold tolerance encoded in one SNP. Cell **160**:1045–1046.

Miao, J., Guo, D., Zhang, J., Huang, Q., Qin, G., Zhang, X., Wan, J., Gu, H., and Qu, L.J. (2013). Targeted mutagenesis in rice using CRISPR-Cas system. Cell Res. **23**:1233–1236.

Mosher, S., Moeder, W., Nishimura, N., Jikumaru, Y., Joo, S.H., Urquhart, W., Klessig, D.F., Kim, S.K., Nambara, E., and Yoshioka, K. (2010). The lesion-mimic mutant *cpr22* shows alterations in abscisic acid signaling and abscisic acid insensitivity in a salicylic acid-dependent manner. Plant Physiol. **152**:1901–1913.

Nawaz, Z., Kakar, K.U., Saand, M.A., and Shu, Q.Y. (2014). Cyclic nucleotide-gated ion channel gene family in rice, identification, characterization and experimental analysis of expression response to plant hormones, biotic and abiotic stresses. BMC Genomics **15**:853.

Pan, Y., Chai, X., Gao, Q., Zhou, L., Zhang, S., Li, L., and Luan, S. (2019). Dynamic interactions of plant CNGC subunits and calmodulins drive oscillatory Ca^{2+} channel activities. Dev. Cell **48**:710–725 e715.

Sanders, D., Pelloux, J., Brownlee, C., and Harper, J.F. (2002). Calcium at the crossroads of signaling. Plant Cell Suppl. **14**:S401–S417.

Sasaki, T., and Burr, B. (2000). International rice genome sequencing project: the effort to completely sequence the rice genome. Curr. Opin. Plant Biol. **3**:138–141.

Stockinger, E.J., Gilmour, S.J., and Thomashow, M.F. (1997). *Arabidopsis thaliana CBF1* encodes an AP2 domain-containing transcriptional activator that binds to the C-repeat/DRE, a *cis*-acting DNA regulatory element that stimulates transcription in response to low temperature and water deficit. Proc. Natl. Acad. Sci. U S A **94**:1035–1040.

Sun, S.J., Qi, G.N., Gao, Q.F., Wang, H.Q., Yao, F.Y., Hussain, J., and Wang, Y.F. (2016). Protein kinase OsSAPK8 functions as an essential activator of S-type anion channel OsSLAC1, which is nitrate-selective in rice. Planta **243**:489–500.

Takabatake, R., Seo, S., Mitsuhara, I., Tsuda, S., and Ohashi, Y. (2006). Accumulation of the two transcripts of the *N* gene, conferring resistance to *tobacco mosaic virus*, is probably important for *N* gene-dependent hypersensitive cell death. Plant Cell Physiol. **47**:254–261.

Thomashow, M.F. (1999). Plant cold acclimation: freezing tolerance genes and regulatory mechanisms. Annu. Rev. Plant Physiol. Plant Mol. Biol. **50**:571–599.

Tian, W., Hou, C., Ren, Z., Wang, C., Zhao, F., Dahlbeck, D., Hu, S., Zhang, L., Niu, Q., Li, L., et al. (2019). A calmodulin-gated calcium channel links pathogen patterns to plant immunity. Nature **572**:131–135.

Tunc-Ozdemir, M., Tang, C., Ishka, M.R., Brown, E., Groves, N.R., Myers, C.T., Rato, C., Poulsen, L.R., McDowell, S., Miller, G., et al. (2013). A cyclic nucleotide-gated channel (CNGC16) in pollen is critical for stress tolerance in pollen reproductive development. Plant Physiol. **161**:1010–1020.

Wang, J., Wu, F., Zhu, S., Xu, Y., Cheng, Z., Wang, J., Li, C., Sheng, P., Zhang, H., Cai, M., et al. (2016). Overexpression of OsMYB1R1-VP64 fusion protein increases grain yield in rice by delaying flowering time. FEBS Lett. **590**:3385–3396.

Wang, J., Liu, X., Zhang, A., Ren, Y., Wu, F., Wang, G., Xu, Y., Lei, C., Zhu, S., Pan, T., et al. (2019). A cyclic nucleotide-gated channel mediates cytoplasmic calcium elevation and disease resistance in rice. Cell Res **29**:820–831.

Wu, Y., Gao, Y., Zhan, Y., Kui, H., Liu, H., Yan, L., Kemmerling, B., Zhou, J., He, K., and Li, J. (2020). Loss of the common immune coreceptor BAK1 leads to NLR-dependent cell death. Proc. Natl. Acad. Sci. U S A **117**:27044–27053.. https://doi.org/10.1073/pnas.1915339117.

Xu, Y., Yang, J., Wang, Y., Wang, J., Yu, Y., Long, Y., Wang, Y., Zhang, H., Ren, Y., Chen, J., et al. (2017). OsCNGC13 promotes seed-setting rate by facilitating pollen tube growth in stylar tissues. PLoS Genet. **13**:e1006906.

Yamaguchi-Shinozaki, K., and Shinozaki, K. (1994). A novel *cis*-acting element in an *Arabidopsis* gene is involved in responsiveness to drought, low-temperature, or high-salt stress. Plant Cell **6**:251–264.

Yoshioka, K., Kachroo, P., Tsui, F., Sharma, S.B., Shah, J., and Klessig, D.F. (2001). Environmentally sensitive, SA-dependent defense responses in the *cpr22* mutant of *Arabidopsis*. Plant J. **26**:447–459.

Yu, I.C., Parker, J., and Bent, A.F. (1998). Gene-for-gene disease resistance without the hypersensitive response in *Arabidopsis dnd1* mutant. Proc. Natl. Acad. Sci. U S A **95**:7819–7824.

Yu, X., Xu, G., Li, B., de Souza Vespoli, L., Liu, H., Moeder, W., Chen, S., de Oliveira, M.V.V., Ariadina de Souza, S., Shao, W., et al. (2019). The receptor kinases BAK1/SERK4 regulate Ca^{2+} channel-mediated cellular homeostasis for cell death containment. Curr. Biol. **29**:3778–3790.e8.

Yuan, P., Yang, T., and Poovaiah, B.W. (2018). Calcium signaling-mediated plant response to cold stress. Int. J. Mol. Sci. **19**:3896.

Zhang, J., Li, X.M., Lin, H.X., and Chong, K. (2019). Crop improvement through temperature resilience. Annu. Rev. Plant Biol. **70**:753–780.

Zhang, Y., Su, J., Duan, S., Ao, Y., Dai, J., Liu, J., Wang, P., Li, Y., Liu, B., Feng, D., et al. (2011). A highly efficient rice green tissue protoplast system for transient gene expression and studying light/chloroplast-related processes. Plant Methods **7**:30.

Zhong, R., Wang, Y., Gai, R., Xi, D., Mao, C., and Ming, F. (2020). Rice SnRK protein kinase *OsSAPK8* acts as a positive regulator in abiotic stress responses. Plant Sci. **292**:110373.

Zhu, J.K. (2016). Abiotic stress signaling and responses in plants. Cell **167**:313–324.